

## INTERPOLATION TECHNIQUE IN DIFFRACTION TOMOGRAPHY

Yoshio Yamaguchi<sup>†</sup>, Masahisa Mochida<sup>†</sup>, Wolfgang -M. Boerner<sup>††</sup>,  
Masakazu Sengoku<sup>†</sup>, Takeo Abe<sup>†</sup>, and Hyo. J. Eom<sup>†††</sup>

<sup>†</sup> : Faculty of Engineering, Niigata University, Niigata, 950-21 Japan

<sup>††</sup> : Department of EECES, University of Illinois at Chicago, IL, USA

<sup>†††</sup> : Department of Electrical Engineering, KAIST, Taejeon, Korea

**1. Introduction** : As regards the improvement of accuracy in the reconstructed image in diffraction Tomography, there are some techniques available such as iterative reconstruction approach, interpolation technique in the frequency domain, etc. Here, we focus our attention to the interpolation technique and examine how the accuracy of reconstructed image change with interpolation technique in diffraction tomography. The interpolation technique in the frequency domain include the nearest neighbor method, bi-linear method [1], and cubic convolution method [2],[3]. In the paper, we show the cubic convolution method is the most effective for improvement of accuracy from the evaluation of relative mean squared error.

**2. Formulation** : Under the Born approximation, the scattered electric field in the free space can be expressed in an integral form as

$$\Psi_s(\mathbf{x}) = k_0^2 \int G(\mathbf{x} - \mathbf{y}) f(\mathbf{y}) \Psi_I(\mathbf{y}) d\mathbf{y} \quad \mathbf{y} \in \text{object} \quad (1)$$

where,  $\Psi_s(\mathbf{x})$  : scattered field,  $\Psi_I(\mathbf{y})$  : incident field,  $f(\mathbf{y})$  : object function,  $G(\mathbf{x} - \mathbf{y})$  : Green's function,  $k_0$  : the free space wave number. From the equation (1), we obtain the following relation between the scattered field and the object function in the Fourier transformed domain.

$$F(\mathbf{u}) = -\frac{2\gamma}{\pi j} \exp(j2\pi\Gamma\gamma) g(\sigma) \quad \mathbf{u} = (\gamma - \alpha)\hat{\mathbf{k}} + \sigma\tilde{\mathbf{k}} \quad (2)$$

where,  $F(\mathbf{u})$  : Fourier transform of the object function,  $g(\sigma)$  : Fourier transform of the scattered field,  $\gamma = \sqrt{\alpha^2 - \sigma^2}$ ,  $\alpha = 1/\lambda$ ,  $\lambda$  : wave length,  $\hat{\mathbf{k}}$ ,  $\tilde{\mathbf{k}}$  : unit vectors parallel, orthogonal to wave propagation,  $\sigma$  : wavenumber in the  $\tilde{\mathbf{k}}$  direction,  $\Gamma$  : distance from the origin to the data line in the space domain (see Fig.1). Therefore, the the object function  $f(\mathbf{y})$  is computed via two-dimensional inverse Fourier transform. In the numerical calculation, we use FFT algorithm for the Fourier transform which utilizes the rectangular coordinate system demanding that the location of sampling points be on rectangular grids, i.e., the sampling data must locate on intersections of rectangular grids. Since the data is located along a semi-circular arc as shown in Fig.2, some interpolation techniques which represents the value on the rectangular grids must be introduced.

**3. Interpolation** : Here, we introduce three interpolation techniques, i.e, nearest neighbor interpolation, bi-linear interpolation, cubic convolution interpolation.

**3-1. Nearest neighbor interpolation method** : This method choose the value on the nearest semi-circular arc as the value on the rectangular grids. The position error becomes a maximum of 1/2 pixel length. This method has an advantage that the algorithm is simple and saves computation time.

**3-2. Bi-linear interpolation method** : The semi-circular arc coordinate system is settled by  $\sigma$  and incidence angle  $\phi$  (Fig.2). This method calculates the value on the rectangular grids by the following equation (3).

$$F(U_1, U_2) = F(\sigma, \phi) = \sum_{i=1}^{N_\sigma} \sum_{j=1}^{N_\phi} F(\sigma_i, \phi_j) h_1(\sigma - \sigma_i) h_2(\phi - \phi_j) \quad \begin{cases} N_\sigma : \text{sample number of } \sigma \\ N_\phi : \text{sample number of } \phi \end{cases} \quad (3)$$

where, the weighting function is expressed as follows.

$$h_1(\sigma) = \begin{cases} 1 - (|\sigma| / \Delta\sigma) & |\sigma| \leq \Delta\sigma \\ 0 & \text{otherwise} \end{cases} \quad (4)$$

$$h_2(\phi) = \begin{cases} 1 - (|\phi| / \Delta\phi) & |\phi| \leq \Delta\phi \\ 0 & \text{otherwise} \end{cases} \quad (5)$$

$\Delta\sigma$ ,  $\Delta\phi$  is the sample interval of  $\sigma$ ,  $\phi$  respectively. This method has the effect of smoothing.

**3-3. Cubic convolution interpolation method** : This is the method which uses the following equation in the weighting function of the equations (4) and (5).

$$h_1(\sigma) = \begin{cases} 1 - 2(|\sigma| / \Delta\sigma)^2 + (|\sigma| / \Delta\sigma)^3 & |\sigma| \leq \Delta\sigma \\ 4 - 8(|\sigma| / \Delta\sigma) + 5(|\sigma| / \Delta\sigma)^2 - (|\sigma| / \Delta\sigma)^3 & \Delta\sigma \leq |\sigma| \leq 2\Delta\sigma \\ 0 & 2\Delta\sigma \leq |\sigma| \end{cases} \quad (6)$$

$$h_2(\phi) = \begin{cases} 1 - 2(|\phi| / \Delta\phi)^2 + (|\phi| / \Delta\phi)^3 & |\phi| \leq \Delta\phi \\ 4 - 8(|\phi| / \Delta\phi) + 5(|\phi| / \Delta\phi)^2 - (|\phi| / \Delta\phi)^3 & \Delta\phi \leq |\phi| \leq 2\Delta\phi \\ 0 & 2\Delta\phi \leq |\phi| \end{cases} \quad (7)$$

The above equation corresponds to the piecewise three-dimensional polynomial approximation of sinc function. The method has the effects of both smoothing and sharpness in imaging.

**4. Numerical simulation** : Consider the case that TM wave is incident on an infinitely long lossless circular cylinder placed in the free space. The relative permittivity is 1.02 and the radius is  $10\lambda$ . The data line  $\Gamma$  is located at  $100\lambda$  behind the cylinder. Three-dimensional displays of the reconstructed permittivities using three interpolation techniques are shown in Fig.3. Fig.4 also shows the vertical cut-views of Fig.3. Both figures represent the characteristics of each interpolation techniques well. For comparison of these image, we examined the relative mean squared error (MSE) using the results similar to those in Fig.3. The MSE as a function of relative permittivity is shown in Fig.5(a), while the MSE as a function of radius of the cylinder is shown in Fig.5(b). As seen in Fig.5, the difference of MSE in the nearest neighbor and the bi-linear techniques increases with increasing relative permittivity. Although the difference in MSE between the bi-linear and the cubic convolution interpolation is small, the cubic convolution technique produce the smallest MSE. On the other hand, the cubic convolution technique sharpens the boundary (see Fig.4). From these considerations, the cubic convolution method seems the most effective for improvement of accuracy in the reconstruction of image in diffraction tomography.

**5. Conclusion** : In this paper, three interpolation techniques for image reconstruction are compared. Among them, the cubic convolution interpolation technique seems the most effective method from the point of relative mean squared error. It will be necessary to introduce cubic convolution interpolation technique into the reconstruction considering multiple scattering and to examine its effect.

## Reference

- [1] S. X. Pan and A. C. Kak, "A computational study of reconstruction algorithms for diffraction tomography : Interpolation versus filtered back propagation", *IEEE Trans. Acoust. Speech Signal Processing*, vol. ASSP - 31, no. 5, pp. 1262 - 1275, 1983.
- [2] M. Oyama, *Image processing handbook*, Syoko-do, pp.273 - 276, 1987.
- [3] M. Takagi, et al. *Handbook of image analysis*, Tokyo university publishing party, pp.441 - 444, 1991.

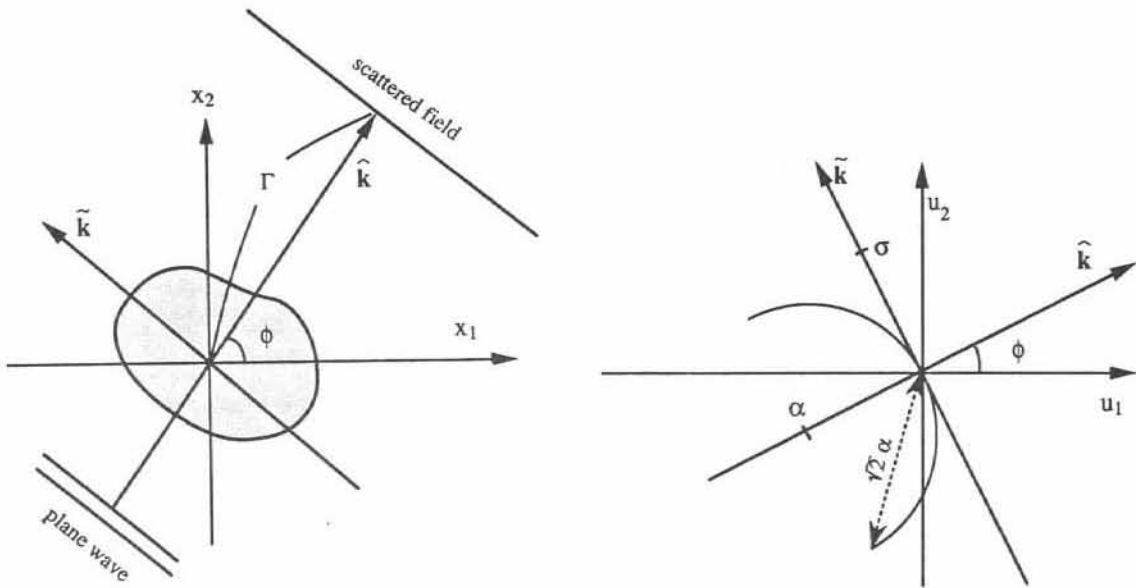
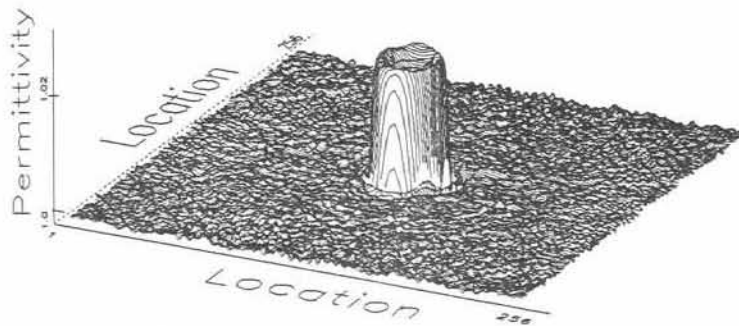
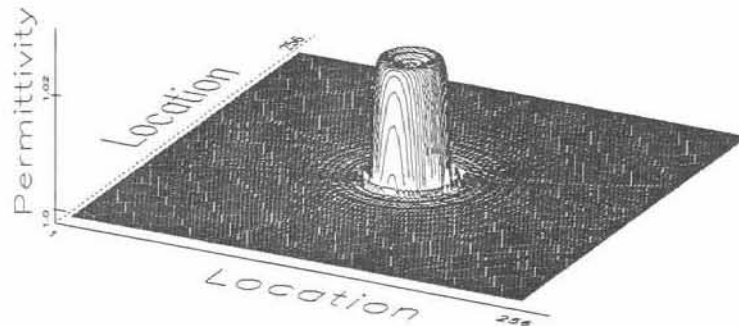


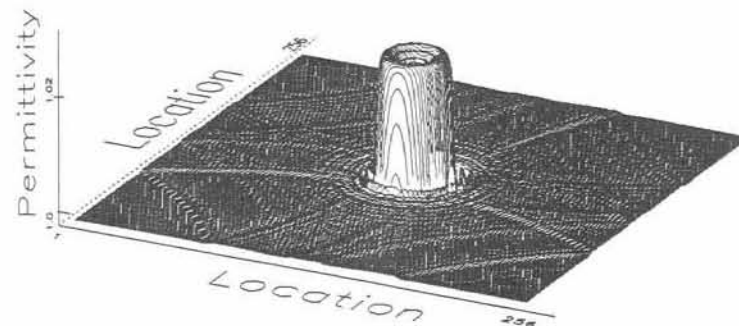
Fig.1 Scattering problem in the space domain Fig.2 The object function in the frequency domain



(a) Nearest neighbor interpolation

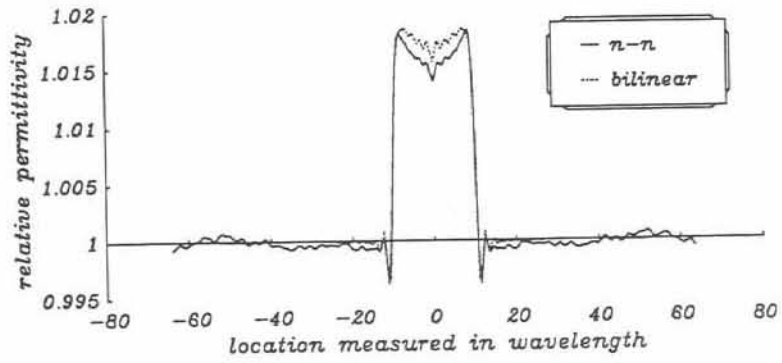


(b) Bi-linear interpolation

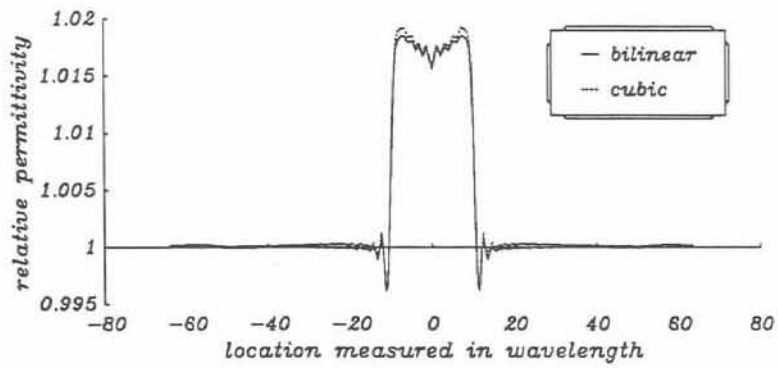


(c) Cubic convolution interpolation

Fig.3 The three-dimensional display of reconstructed permittivity

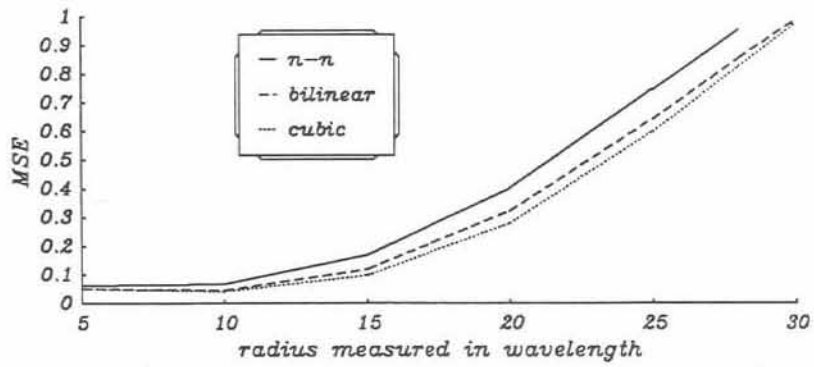


(a) Nearest neighbor interpolation and bi-linear interpolation

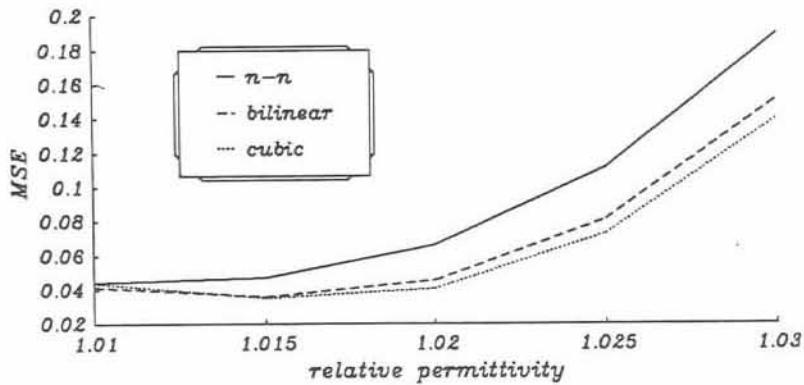


(b) Bi-linear interpolation and cubic convolution interpolation

Fig.4 The vertical cut-view image



(a) Relative permittivity - MSE distribution



(b) Radius - MSE distribution

Fig.5 The comparison of MSE